Control of Stem Cell Self-Renewal in *Drosophila* Spermatogenesis by JAK-STAT Signaling

Natalia Tulina and Erika Matunis*

Stem cells, which regenerate tissue by producing differentiating cells, also produce cells that renew the stem cell population. Signals from regulatory microenvironments (niches) are thought to cause stem cells to retain self-renewing potential. However, the molecular characterization of niches remains an important goal. In *Drosophila* testes, germ line and somatic stem cells attach to a cluster of support cells called the hub. The hub specifically expresses Unpaired, a ligand activating the JAK-STAT (Janus kinase–signal transducer and activator of transcription) signaling cascade. Without JAK-STAT signaling, germ line stem cells differentiate but do not self-renew. Conversely, ectopic JAK-STAT signaling greatly expands both stem cell populations. We conclude that the support cells of the hub signal to adjacent stem cells by activation of the JAK-STAT pathway, thereby defining a niche for stem cell self-renewal.

A small population of germ line stem cells (GSCs) in a morphologically well-defined environment sustains *Drosophila* spermatogenesis (*1*). GSCs attach to a cluster of nonmitotic somatic support cells at the testis apex, called the hub (Fig. 1A). GSC divisions are asymmetric, producing GSCs remaining at the hub as well as differentiating daughters (gonialblasts) displaced away from the hub. Recently, a somatic signal regulating the GSC lineage was found. Although the identity of this signal is unknown, it promotes the GSC-to-gonialblast transition (*2, 3*). We hypothesized that an opposing signal, likely produced by hub cells, should promote GSC self-renewal.

We found that Unpaired (Upd), a secreted ligand activating the highly conserved JAK-STAT signaling pathway (*4*), is expressed specifically in hub cells (Fig. 1, B and C). Upd signals through the recently identified receptor Domeless (*5*), activating the JAK kinase homolog Hopscotch (Hop) and the STAT homolog Stat92E, which enters the nucleus to activate target genes (*6*). Localized expression of Upd by hub cells suggests that Upd activates the JAK-STAT pathway in adjacent stem cells.

To test this possibility, we analyzed the effects of removing Hop and Stat92E on stem cells. In contrast to the wild type, testes from the male-sterile, partial loss-of-function mutant *hop[25]* (*7*) contain hub cells but lack stem cells and spermatogonia (Fig. 2, A and B). Analysis of markers for the hub and either stem cell lineage (*8*) in *hop[25]* testes (*9*), and of *hop[2]* (null) testes (Fig. 2, C and D) (*10*), confirms that Hop maintains GSCs and somatic stem cells (SSCs). Because Stat92E is similarly required (see below), we suggest that Upd, signaling through JAK-STAT, maintains either the self-renewing capacity or viability of GSCs and SSCs.

We next determined whether Upd signals directly to GSCs, and whether it instructs GSC self-renewal or maintains GSC viability. For example, if Upd maintains GSC viability, GSCs lacking Hop or Stat92E (and thus unable to transduce the signal) would not survive or produce progeny. Conversely, if Upd instructs GSC self-renewal, GSCs unable to transduce the signal would survive but would produce spermatogonia rather than replenish the GSC population. To create GSCs unable to respond to Upd, we induced *stat92E* null clones (*11*). Two days later (day 2), *stat92E* GSCs were frequently detected (Fig. 2E). However, *stat92E* GSCs were rare by day 5 and were absent by day 9, whereas control GSC clones remained. A different strong loss-of-function allele of *stat92E* yielded similar results (Table 1). The finding that *stat92E* GSCs are initially seen but do not persist shows that Stat92E is required directly in the germ line for GSC maintenance.

To distinguish whether Stat92E maintains GSC self-renewal or viability, we tested whether *stat92E* GSCs were chased into spermatogonia. Because gonialblasts become spermatocytes in about 2 days, marked spermatogonia present at day 5 originate from marked GSCs. *stat92E* spermatogonia are found in 48% (14/29) of testes at day 5 (Fig. 2F). A similar number of spermatogonial clones (41%, 9/22) is detected in day 5 control testes. Because progeny of *stat92E* GSCs differentiate rather than die, JAK-STAT signaling is required in the germ line for

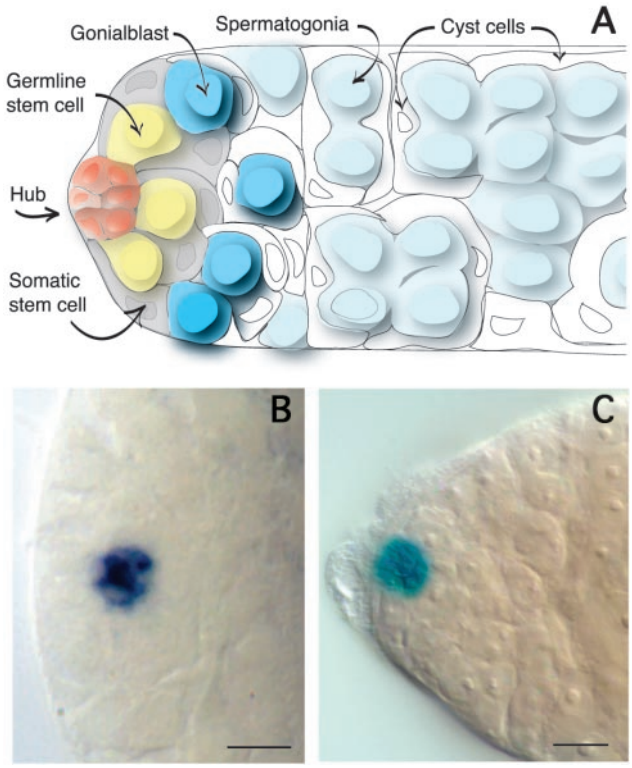

Fig. 1. The ligand Upd is specifically expressed in the hub. (**A**) The *Drosophila* testis apex. Germ line stem cells (five to nine cells; yellow) attach to a cluster of about 12 somatic hub cells (red). GSC daughters adjacent to the hub remain stem cells (yellow); daughters displaced from the hub differentiate into gonialblasts (blue). Gonialblasts undergo four synchronous, incomplete mitotic divisions, forming 16 interconnected spermatogonia (light blue; cysts representing the first, second, and third divisions are shown). Later, spermatogonia exit mitosis and enter meiosis, becoming spermatocytes. Cells move progressively further from the apex as differentiation proceeds. Each gonialblast and its progeny are enveloped by two somatic support cells throughout spermatogenesis (cyst cells, colorless) arising from asymmetric divisions of cyst progenitor cells (herein termed SSCs, gray). (**B**) In situ hybridization to whole adult testes (*3*); *Upd* mRNA (*4*) is localized to the cells of the hub. (**C**) X-gal activity stain (*26*); an enhancer detector inserted in *Upd* (*27*) is expressed in the hub. Apical is to the left in all panels. Scale bars, 10 μm.

Department of Embryology, Carnegie Institution of Washington, 115 West University Parkway, Baltimore, MD 21210, USA.

*To whom correspondence should be addressed. E-mail: matunis@ciwemb.edu

GSC self-renewal rather than for GSC viability.

If JAK-STAT signaling alone promotes stem cell self-renewal, then ectopic signaling could increase the GSC population. To test this possibility, we used the binary GAL4/UAS system to overexpress Upd (*12*). The proliferation center in wild-type testes is restricted to the apex. About half (43/91) of the testes ectopically expressing Upd have a striking accumulation of early-stage cells distant from the hub (compare bracketed areas, Fig. 3, A and B). By their morphology and DNA staining characteristics, these cells are a mixture of undifferentiated germ line and somatic cells. This interpretation was confirmed by examining the fusome, a germ cell–specific organelle that is spherical in GSCs and gonialblasts (*13*). Typically, GSCs are connected to gonialblasts by a cytoplasmic bridge (*14*); the fusome occupies the bridge. In contrast, spermatogonia have branched fusomes (compare arrow and arrowhead, Fig. 3C). In testes expressing Upd ectopically, the number of cells with spherical fusomes increases markedly over the wild-type number of about 12. Typically, in a field of several hundred ectopic early germ cells, two-thirds of the cells have spherical fusomes. The fusomes are often located in the cytoplasmic bridge between the GSC and gonialblast, as in the wild type (compare arrows, Fig. 3, C and D), indicating that the GSC and/or gonialblast population is greatly expanded. This was verified by analyzing Bag-of-marbles (Bam) expression, which marks two-, four-, and eight-cell spermatogonial cysts (Fig. 3E) (*15*). Testes expressing ectopic Upd contain a greatly increased number of germ cells lacking Bam (Fig. 3F), consistent with a GSC and/or gonialblast identity. This finding was confirmed by simultaneously analyzing fusome morphology and Bam expression. Bam-negative germ cells have spherical fusomes (*9*). The population of Bam-positive spermatogonia also expands (Fig. 3F, arrow). These cells likely derive from excess gonialblasts as they differentiate, whereas the gonialblasts derive from excess GSCs. We conclude that ectopic Upd is sufficient to expand the GSC population.

In addition to excess GSCs, gonialblasts, and spermatogonia, testes with ectopic Upd contain excess undifferentiated somatic cells (Fig. 3D, arrowhead). This was confirmed using the late interphase marker Anillin, which strongly stains SSCs but decreases as cyst cells differentiate (compare small and large arrowheads, Fig. 3H) (*16*). In testes expressing Upd ectopically, ectopic Anillin-positive somatic cells are observed (Fig. 3I), consistent with a SSC identity. Occasionally, Anillin is observed cortically, a distribution that occurs only during M phase; hence, these somatic cells are cycling (Fig. 3I, arrow). Because the only cycling somatic cells in wild-type testes are SSCs (Fig. 3H, arrow), this is also consistent with a SSC identity. Conversely, Eyes-absent (*17*) and S359 (*8*), which mark cyst cells rather than SSCs, are not expressed in ectopic somatic cells (*9*). We conclude that the SSC population expands when Upd is ectopically expressed. Ultrastructural analysis of these cells reveals somatic cells (Fig. 3G, SC) encircling GSC and/or gonialblast pairs (Fig. 3G, GP). This intimate association between GSCs and SSCs is similar to that observed in the wild type (*14*), which suggests that close contact between the two lineages coordinates the expansion of both stem cell populations. Because activation of the Upd-JAK-STAT pathway is sufficient to generate excess stem cells in both lineages, we conclude that Upd normally instructs GSCs and SSCs to undergo self-renewal.

These data reveal a molecular mechanism governing stem cell self-renewal in a stem cell niche in vivo. We conclude that in the *Drosophila* testis, hub cells are a localized source of the ligand Upd, which activates the JAK-STAT pathway in adjacent stem cells. This signaling ensures that GSCs and SSCs attached to the hub undergo self-renewal while daughter cells that are displaced away from the niche differentiate. Perhaps cells displaced from the hub do not receive sufficiently high levels of Upd to activate the JAK-STAT pathway, and therefore lose self-renewing capacity. This decision to differentiate is reinforced by a subsequent signal, relayed to the gonialblast from the cyst cell lineage, that promotes the transition from GSC

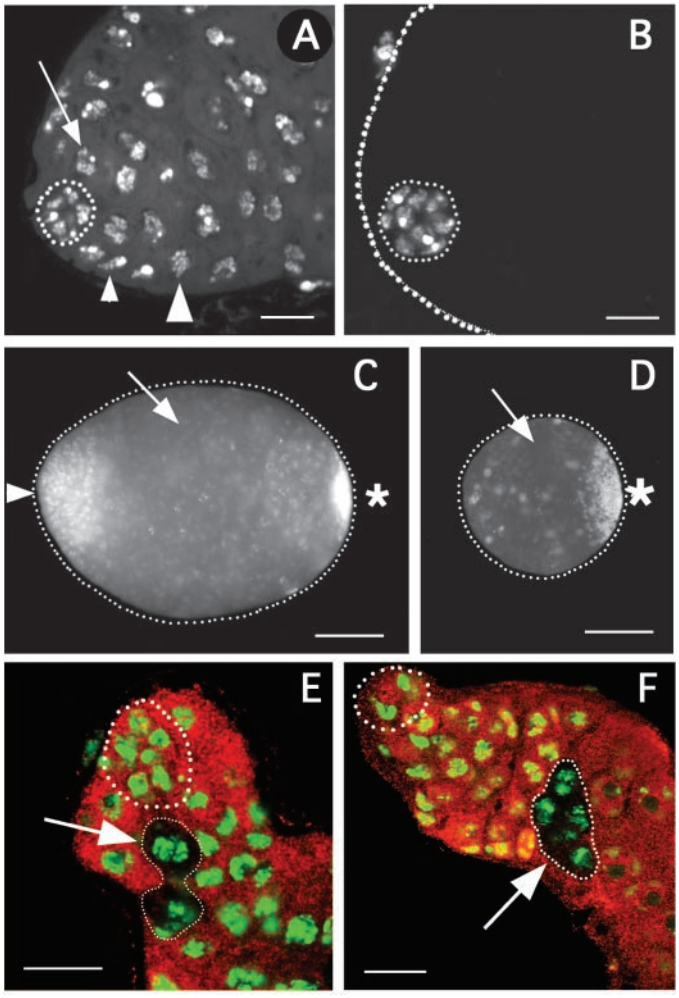

Fig. 2. JAK-STAT signaling is required for germ line stem cell self-renewal. (**A** and **B**) Confocal section through the apical region of adult testes stained for DNA. In a wild-type testis (A), nuclei of hub cells (outlined), GSCs (arrow), SSCs (small arrowhead), and spermatogonia (large arrowhead) are visible. In a *hop[25]* testis (B), only hub cells remain (narrow outline); heavy outline denotes testis edge. (**C** and **D**) DNA-stained whole third-instar larval testes. A wild-type testis (C) shows brightly staining GSCs and spermatogonia at the apex (arrowhead), diffusely staining spermatocytes distal from the apex (arrow), and brightly staining terminal epithelial cells at the basal end (asterisk). A *hop[2]* testis (D) is much smaller than in the wild type; notably, GSCs and spermatogonia are absent. A few spermatocytes (arrow) and terminal epithelial cells (asterisk) remain. (**E** and **F**) Confocal sections through the apex of testes containing *stat92E* clones at day 5. Wild-type cells are marked by a nuclear and cytoplasmic signal (red); unmarked cells are null for *stat92E* but are visible by DNA counterstain (green). In (E), a *stat92E* null GSC-gonialblast pair (arrow) is at the hub (outlined). In (F), *stat92E* null spermatogonia (arrow) are distal from the hub (outlined). Scale bars, 100 μm [(C) and (D)], 10 μm (other panels).

Table 1. *stat92E* null GSCs are not maintained.

Days after induction	Stat92E allele	Testes with GSC clone/ testes scored
2	Wild type	11/20 (55%)
2	06346	9/26 (35%)
2	l(3)J6C8	10/21 (48%)
3	Wild type	8/25 (32%)
3	06346	6/24 (25%)
3	l(3)J6C8	4/20 (20%)
5	Wild type	42/87 (48%)
5	06346	3/79 (4%)
5	l(3)J6C8	0/20 (0%)
9	Wild type	9/24 (38%)
9	06346	0/20 (0%)
9	l(3)J6C8	0/20 (0%)

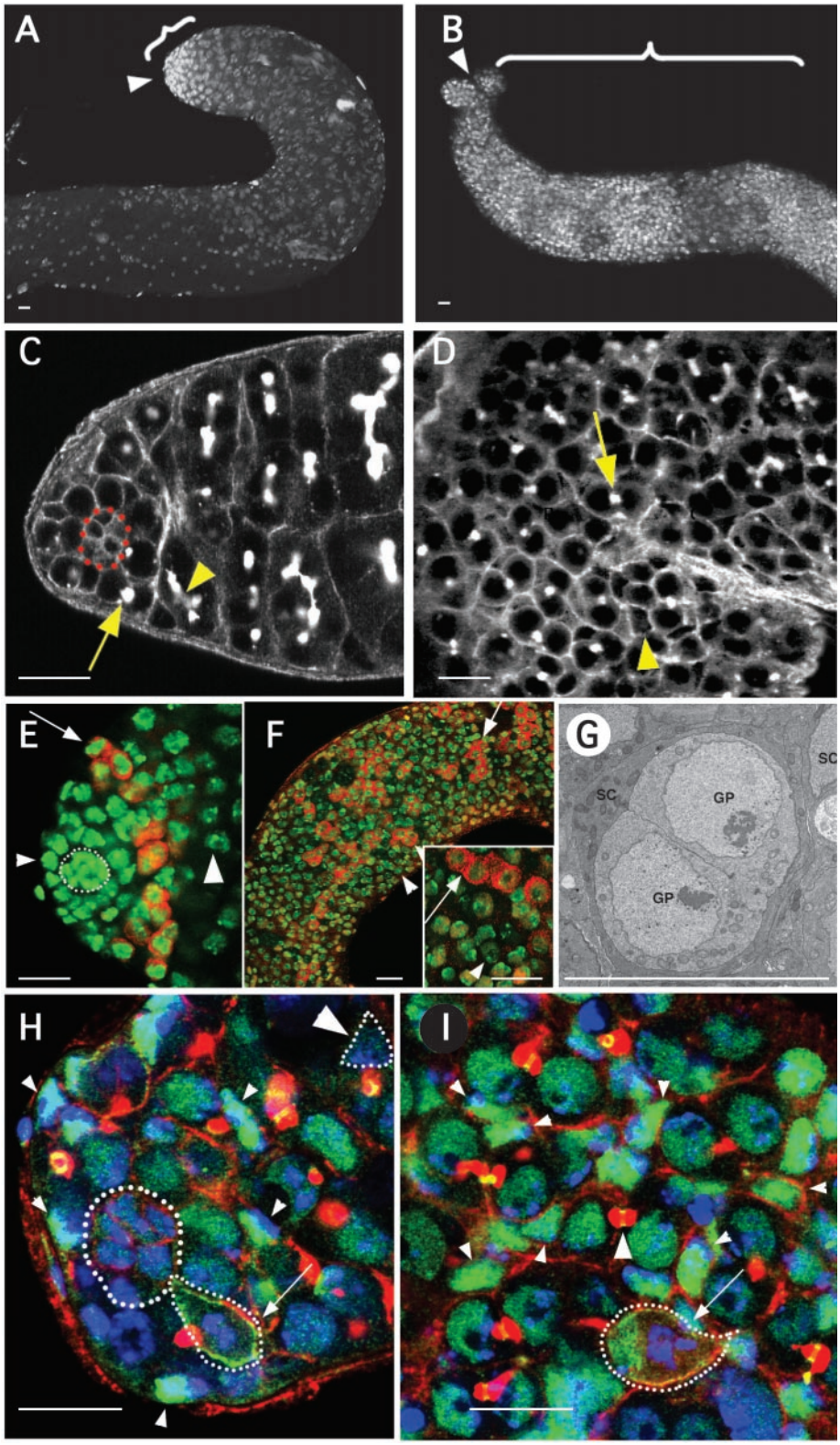

Fig. 3. Ectopic JAK-STAT signaling expands the germ line and somatic stem cell populations in adult testes. (**A** and **B**) DNA stain; arrowhead indicates apex. In (A), a wild-type testis contains a small domain of brightly staining GSCs and spermatogonia (bracket); weakly staining spermatocytes are distal from this domain. In (B), ectopic Upd greatly expands the domain of brightly staining cells (bracket) into the region of the testis normally containing spermatocytes. (**C** and **D**) Fusome morphology. In (C), a wild-type GSC-gonialblast pair at the hub (red outline) contains a spherical fusome (arrow); a cyst of spermatogonia contains a branching fusome (arrowhead). In (D), ectopic Upd produces ectopic GSC-gonialblast pairs with spherical fusomes (arrow); somatic cells are also generated (arrowhead). (**E** and **F**) Bam expression (red) and DNA (green). In (E), cytoplasmic Bam in the wild type is present in mitotic spermatogonia (arrow), absent from GSCs (small arrowhead) at the hub (outlined), and absent from spermatocytes (large arrowhead). In (F), ectopic Upd expands Bam-positive (arrow) and Bam-negative (arrowhead) germ cell populations, magnified in the inset. (**G**) A testis expressing ectopic Upd; somatic cells (SC) envelop an ectopic GSC-gonialblast pair (GP). (**H** and **I**) Anillin expression (green), fusomes (red), and DNA (blue). In (H), Anillin marks all interphase nuclei in the wild type, particularly SSC nuclei (small arrowheads) near the hub (outlined). Their nonmitotic progeny (cyst cells) lack Anillin (outlined; large arrowhead). At metaphase, Anillin is cortical; an SSC is outlined (arrow). Anillin also marks ring canals (yellow, due to colocalization with fusomes, red). In (I), ectopic Upd expands the Anillin-positive somatic cell population (small arrowheads); one in mitosis is outlined (arrow). Fusomes with one ring canal (large arrowhead) indicate ectopic GSC-gonialblast pairs. Ectopic Upd produced by SSCs [(B) and (D)] or GSCs [(F), (G), and (I)] gives indistinguishable phenotypes. All panels show confocal sections except (G), which is an electron micrograph. Scale bars, 10 μm.

to gonialblast. Although the differentiation signal is currently unidentified, its production requires activation of mitogen-activated protein (MAP) kinase in the soma (*2, 3*). An intriguing parallel to this emerging pathway in stem cell self-renewal is a requirement for JAK-STAT signaling in the maintenance of mammalian embryonic stem (ES) cells (*18*). The JAK-STAT signal is counterbalanced by the requirement for MAP kinase activation, which promotes ES cell differentiation (*19*). Because of these parallels, genetic identification of targets of the JAK-STAT signaling pathway in *Drosophila* germ line and somatic stem cells holds great potential for revealing the molecular basis of stem cell self-renewal in more complex systems.

References and Notes

1. M. T. Fuller, *Development of* Drosophila melanogaster (Cold Spring Harbor Laboratory Press, Cold Spring Harbor, NY, 1993), vol. 1, pp. 71–147.

2. J. Tran, T. J. Brenner, S. DiNardo, *Nature* **407**, 754 (2000).
3. A. A. Kiger, H. White-Cooper, M. T. Fuller, *Nature* **407**, 750 (2000).
4. D. A. Harrison, P. E. McCoon, R. Binari, M. Gilman, N. Perrimon, *Genes Dev.* **12**, 3252 (1998).
5. S. Brown, N. Hu, J. Castelli-Gair Hombría, *Curr. Biol.* **11**, 1700 (2001).
6. M. P. Zeidler, E. A. Bach, N. Perrimon, *Oncogene* **19**, 2598 (2000).
7. N. Perrimon, A. P. Mahowald, *Dev. Biol.* **118**, 28 (1986).
8. P. Gönczy, thesis, Rockefeller University (1995).
9. E. Matunis, N. Tulina, data not shown.
10. R. Binari, N. Perrimon, *Genes Dev.* **8**, 300 (1994).
11. Germ line clones homozygous for stat92E$^{l(3)J6C8}$ or stat92E^{06346} (*20*) were induced in *yw P[ry+;hsp70 FLP]^{12}/Y; P[hs-neo; ry+;FRT]82B, arm LacZ/ P[hs-neo; ry+;FRT]82B, P[mini w+; l(3)J6C8]* and *yw P[ry+; hsp70 FLP]12/Y; mrl P1681, P[hs-neo; ry+;FRT]82B/ P[ry+;hsp70 FLP]12; P[hs-neo; ry+;FRT]82B, arm LacZ* adult males heat-shocked twice at 37°C for 30 min.
12. Ectopic Upd was generated in GSCs and spermatogonia by expressing UAS-Upd (*4*) with a Nanos-Gal4 driver (*21*) (genotype *w/Y; P[w+, UAS Upd]/P[w+, Actin5c>y+>Gal4].P[w+, UAS nGFP]; P[w+; A4-1Nos-Gal4::VP16nos.UTR]/+*), or in SSCs and their progeny by inducing theActin5c promoter (*22*) according to (*23*). Males were heat-shocked twice at 37°C for 30 min, then aged 2 weeks at 25°C (genotype: *w/Y; P[w+, UAS Upd]/Actin5c>CD2>GAL4,UAS GFP; MKRS, P[ry+;hsp70 FLP]/+*), yielding indistinguishable results. Rabbit antibody to β-galactosidase (Abcam, diluted 1:2000), mouse monoclonal antibody 1B1 (DSHB, 1:50), mouse antibody to Eya (DSHB, 1:1000), and mouse antibody to BamC (1:2000) were used as described (*24*). Rabbit antibody to Anillin (1:1000) was used similarly, except that fixation was for 5 min; incubation in secondary antibody was followed by fixation for 30 min. DNA was counterstained with Oligreen (Molecular Probes, 1:4000) for 10 min, or with Toto-3 (Molecular Probes, 1:2000) for 20 min after treatment with ribonuclease A (0.04 mg/ml) for 30 min. Alexa 488– or Alexa 568–conjugated secondary antibodies were used (Molecular Probes, 1:400). Confocal images were obtained with Leica TCS NT and SP2 microscopes.
13. H. Lin, L. Yue, A. C. Spradling, *Development* **120**, 947 (1994).
14. R. W. Hardy, K. T. Tokuyasu, D. L. Lindsley, M. Garavito, *J. Ultrastruct. Res.* **69**, 180 (1979).
15. D. McKearin, B. Ohlstein, *Development* **121**, 2937 (1995).
16. G. R. Hime, J. A. Brill, M. T. Fuller, *J. Cell. Sci.* **109**, 2779 (1996).
17. M. Boyle, N. Bonini, S. DiNardo, *Development* **124**, 971 (1997).
18. T. Matsuda *et al.*, *EMBO J.* **18**, 4261 (1999).
19. A. G. Smith, *Dev. Biol.* **235**, 289 (2001).
20. X. S. Hou, M. B. Melnick, N. Perrimon, *Cell* **84**, 411 (1996).
21. M. Van Doren, A. L. Williamson, R. Lehmann, *Curr. Biol.* **8**, 243 (1998).
22. T. P. Neufeld, A. F. de la Cruz, L. A. Johnston, B. A. Edgar, *Cell* **93**, 1183 (1998).
23. A. H. Brand, N. Perrimon, *Development* **118**, 401 (1993).
24. E. Matunis, J. Tran, P. Gönczy, K. Caldwell, S. DiNardo, *Development* **124**, 4383 (1997).
25. A. A. Kiger, D. L. Jones, C. Schulz, M. B. Rogers, M. T. Fuller, *Science* **294**, 2542 (2001).
26. P. Gönczy, S. Viswanathan, S. DiNardo, *Development* **114**, 89 (1992).
27. Y. C. Tsai, Y. H. Sun, *A. Dros. Res. Conf.* **42**, 585C (2001).
28. We thank D. Harrison, H. Sun, C. Dearolf, A. Spradling, S. DiNardo, and the Bloomington Stock Center for flies; C. Field, D. McKearin, and the Developmental Studies Hybridoma Bank for antibodies; M. Sepanski for electron microscopy; and S. DiNardo, M. Halpern, and A. Spradling for helpful comments. We thank M. Fuller for discussing similar findings (*25*). Supported by NIH grant R01HD40307 (E.M.).

1 October 2001; accepted 13 November 2001

Human Appropriation of Photosynthesis Products

Stuart Rojstaczer,* Shannon M. Sterling, Nathan J. Moore

Previous global estimates of the human impact on terrestrial photosynthesis products depended heavily on extrapolation from plot-scale measurements. Here, we estimated this impact with the use of recent data, many of which were collected at global and continental scales. Monte Carlo techniques that incorporate known and estimated error in our parameters provided estimates of uncertainty. We estimate that humans appropriate 10 to 55% of terrestrial photosynthesis products. This broad range reflects uncertainty in key parameters and makes it difficult to ascertain whether we are approaching crisis levels in our use of the planet's resources. Improved estimates will require high-resolution global measures within agricultural lands and tropical forests.

Human use of photosynthesis products is pervasive, including direct use of plants for food and fiber as well as indirect use from grazing by domesticated animals. Population increases have led to speculation and estimates that the human footprint on the biosphere, in terms of the use of both plants and fresh water, is approaching the limit of planet sustainability (*1–5*). A key measure of human impact on the biosphere and hydrosphere is human use of terrestrial net primary production (TNPP), which represents the net energy (production minus respiration) created by carbon fixation on land. Previous estimates of global human appropriation of this biological resource (HTNPP)—which governs the total amount of food available on Earth—and its surrogates (*1, 6–8*) have used mean estimates of parameters that were made on the basis of limited, small-scale field studies. Here we incorporate contemporary data, many of which are satellite-based, to estimate HTNPP, and quantify the uncertainty in our knowledge of HTNPP.

HTNPP represents the combined effects of direct human use and use by human-altered ecosystems (*9*). We adopted the method of Vitousek *et al.* (*1*) to estimate HTNPP (Table 1 and Fig. 1), which uses global averages and sums the influences of agriculture, human-occupied lands, grazing, and forestry. To estimate HTNPP, we used available global-scale primary-source data in the literature (*10*). We did not include studies earlier than 1990 for parameters with large temporal variability (e.g., parameters dependent on areas or populations). We also removed estimates that appeared to be highly anomalous (more than two standard deviations from the other estimates). Reflecting the format of Vitousek *et al.* (*1*) and the majority of data sources, we present biomass and productivity values in terms of the weight of dry matter (DM). Conversion of data from weight carbon (C) to DM included a 10% uncertainty in carbon content (0.45 to 0.50 g C per g DM), reflecting commonly cited carbon values (*11–16*).

We estimated uncertainty for parameters with only one or two literature references using either literature-cited values or an ad hoc estimate that the standard deviation was one-half of the mean (*17, 18*). Although 8 of 34 parameters are estimated with a single measurement, the median number of measurements per parameter is 5.5, indicating that half of the parameters have enough independent measurements to provide at least rudimentary evaluation of their uncertainty. Only nine parameters have normalized 2σ error bounds less than unity, indicating that most parameters are not well known. Uncertainty in our parameters, however, does not significantly increase and correlate with sample size ($r^2 = 0.10$ for estimates using three or more samples), which reflects the fact that the literature-based estimates we used are derived, either directly or indirectly, from physical measurements. Differences between our mean estimates and those of Vitousek *et al.* (*1*) represent updates using newer literature. Coincidentally, the median difference for all 34 of the parameters is negligible, –1.2%.

In addition to using more contemporary and larger scale measurements, we explicitly incorporated uncertainty in our estimate of HTNPP through stochastic simulations. Monte Carlo techniques allow each parameter to randomly vary constrained by its mean and estimated variance. We derived an estimate of variability in our knowledge of HTNPP by repeating these calculations 1 million times (*19*).

Our mean estimate of HTNPP is 39 Pg DM (20 Pg C, where we assume carbon is 50% of dry matter) (Fig. 2) or 32% of TNPP (*20*), which almost precisely matches that of Vitousek *et al.* (*1*). This agreement is coincidental because our newer estimates of the parameters are considerably different from those of Vitousek *et al.* The mean absolute difference between our estimate of the contributing parameters and those of Vitousek *et al.* is, excluding the values for four

Center for Hydrologic Science and Division of Earth and Ocean Sciences, Duke University, Durham, NC 27708, USA.

*To whom correspondence should be addressed. E-mail: stuart@duke.edu